

Thermomechanical response of a viscoelastic beam under cyclic bending; self-heating and thermal failure

F. DINZART¹⁾, A. MOLINARI²⁾, R. HERBACH³⁾

¹⁾ *Laboratoire de Fiabilité Mécanique
57045 Metz, France*

²⁾ *Laboratoire de Physique et Mécanique des Matériaux
Université Paul Verlaine
57045 Metz, France*

³⁾ *Université de Technologie de Belfort–Montbéliard
Sévenans, 90010 Belfort, France*

THE THERMOMECHANICAL RESPONSE of beams made up of thermoplastic polymer is analysed in the case of cyclic bending. The material behavior is modelled by a viscoelastic law depending on temperature and frequency. Inertia effects are neglected. The stress, strain and temperature distributions are expressed as functions of the beam geometry, the loading parameters and the material characteristics. The stability of the steady-state solutions is analysed with use of a linear perturbation approach. The conditions for thermal runaway (thermo-mechanical instability) are explored.

Key words: viscoelastic beam, cyclic bending, self heating, stability analysis, thermal runaway.

1. Introduction

THE DYNAMIC RESPONSE of polymeric materials is of great interest to design such structural elements as vibration dampers and to anticipate catastrophic self-heating, which may occur under particular conditions. Thermal runaway results from unbalance between the loss energy and heat transfer; this phenomenon is worsed by high temperature sensitivity and low thermal conductivity of thermoplastic elastomers.

Experimental aspects of thermal failure in polymers have been explored by HERTZBERG [5], RATNER and KOBOROV [8] and RIDELL *et al.* [9] MENGES and ALF [7] showed the continuous increase of temperature in the case of pulsating tensile load. CONSTABLE [1] explored the cyclic torsion and bending; he related the cyclic thermal softening to the compliance loss, the specimen geometry and the magnitude of cyclic load.

HUANG and LEE [6] studied the thermomechanical coupling phenomena of viscoelastic rods loaded alternatively. TAUCHERT [18] analysed the influence of testing conditions on the internal heat generated in polyethylene rods and showed the existence of high-frequency regime, leading to thermal failure before the thermal equilibrium. TING [19] for alternative torsion solicitation and TING and TUAN [20] for cyclic internal pressure, proposed with use of complex variables, a simplified formulation of the coupled thermomechanical problem. They calculated by iteration the temperature distribution and the stress response describing the equilibrium state.

TAKAHARA *et al.* [10, 11] have calculated the temperature field by assuming a uniform distribution through the sample. LESIEUTRE and GOVINDSWAMY [15] determined the dynamic response in simple shear through generic damping elements introduced in finite element calculation. The temperature effects were introduced owing to a time-dependent shift factor. This description, in terms of reduced time, was also developed by WINEMAN and KOLBERG [21] to determine the continuous response of a polymeric beam subjected to pure bending. SCHAPERY [16] and SCHAPERY and CANTEY [17] studied the thermal response of a viscoelastic material subjected to harmonic shearing for two loading situations: imposed displacement or inertial driving. They have shown the existence of an instable response of the system in accordance with their experimental observations of thermal runaway. Considering the frequency and temperature dependence of viscoelastic materials, the temperature distribution has been obtained in closed form by MOLINARI and GERMAIN [12] for a cyclic compressive loading. They also analysed the stability of the steady state solutions and corroborated the conditions of thermal runaway to experimental observations, see also LEROY and MOLINARI [13] and [14] for analogies with shear stability problems. Using the same thermosensitive law as in [12], DINZART and MOLINARI [3] extended the previous study to torsional loading of plain or hollow cylinders.

This paper is devoted to the analysis of the thermomechanical response of a viscoelastic beam under cyclic pure bending. The classical assumptions of beam theory are made, i.e. plane sections remain plane so that the strains vary linearly through the thickness of the beam. Thermal runaway is explored for a beam under curvature control or under bending moment control. The bending moment and curvature are expressed as functions of the cross-section geometry, the material parameters and loading conditions. The linear viscoelastic behavior is specified as a Boltzmann law, where the storage and loss moduli depend linearly on the temperature. The material is assumed to be isotropic and incompressible. An example of real material is provided by thermoplastic elastomer whose Poisson's ratio is close to 0.5. Inertia effects are neglected. The formulation is restricted to conditions of small strains and rotations; thermal expansion is not taken into account.

The paper is organised as follows. The governing equations and the description of pure bending assumptions are introduced in Sec. 2. The mean temperature over a cycle and the bending moment are expressed as functions of the strain amplitude in Sec. 3. The fourth section is devoted to a parametric study. The conditions of existence of steady-state solutions are established in the last section. A simplified linear stability analysis is conducted under the assumption of uniform temperature distribution, which leads to closed-form conditions of thermal runaway.

2. Governing equations

2.1. Geometry and mechanical fields

The sample is a straight cylindrical beam of rectangular cross-section of characteristic half-height e and half-width l . The x -axis coincides with the line drawn through the centroids of the cross-sections. The y -axis and z -axis are placed along the lines of symmetry. The beam is loaded only by bending moments $M(t)$ about the z -axis at the end faces A and B . The intersection of the beam segment with the $x - y$ plane of symmetry is described in Fig. 1 for undeformed and deformed states.

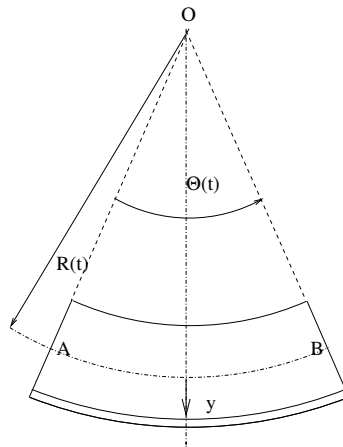
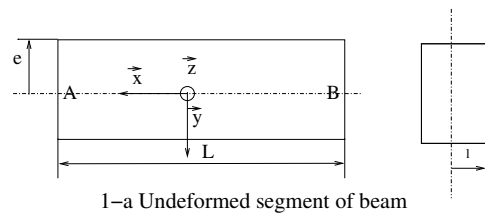


FIG. 1. Geometrical description of the beam.

Standard assumptions concerning pure bending deformation are applied at each time t . The deformation is small enough to neglect the change in shape of the cross-section. Each plane cross-section rotates about the z -direction and remains plane. The line segments initially straight along the y -axis rotate into radial line segments which may intersect at the common point O . The line segments initially straight along the x -axis are curved into circular arcs of center O . These segment lines are alternatively elongated and shorten.

The neutral axis is at the distance $R(t)$ from the center of curvature O . The inclination angle between the end faces A and B is denoted $\Theta(t)$. As the length L of the beam along the neutral axis remains constant, the curvature is related to the inclination angle by

$$(2.1) \quad R(t)\Theta(t) = L.$$

Taking advantages of the symmetry of the problem and of the isotropic behavior of the material, the strain and stress distributions and the temperature do not depend on the spatial variables (x, z) . A local description of the cross-section along the normal direction \mathbf{e}_y is provided by the variable

$$y = r - R(t),$$

where r is the coordinate of a line segment from the center O .

Mechanical boundary conditions

The first type of loading conditions considered in this paper consists in prescribing the rotation angle $\Theta(t)$ in the form of superposition of a periodic loading to a static deformation Θ_m :

$$(2.2) \quad \Theta(t) = \Theta_m + \Theta_0 \sin \omega t$$

with $\Theta_0 \geq 0$.

Alternatively, a second type of loading is analysed when the beam is loaded by a bending moment applied to the end face B :

$$(2.3) \quad M(t) = M_m + M_0 \sin \omega t$$

with $M_0 \geq 0$. The opposite bending moment is applied at the end face A . The inclination angle $\Theta(t)$ is then controlled by the prescribed moment. The curvature or the bending moment are transmitted with no normal resultant force acting on a cross-section and without shearing.

Strain and stress fields

The stress tensor is expressed in the following form:

$$(2.4) \quad \sigma_{ij} = -p\delta_{ij} + s_{ij},$$

where p is the hydrostatic pressure and s_{ij} the stress deviator. The linear isotropic incompressible viscoelastic behavior is described according to the Boltzmann law:

$$(2.5) \quad s_{ij} = 2 \int_{-\infty}^t G(t-t', T) \dot{\varepsilon}_{ij}(t') dt \\ = 2G_{\infty}(T) \varepsilon_{ij} + 2 \int_{-\infty}^t (G(t-t', T) - G_{\infty}(T)) \dot{\varepsilon}_{ij}(t') dt,$$

where $G_{\infty}(T)$ is the equilibrium modulus at the temperature T . The thermal effects are included in the temperature-dependence of the relaxation function G .

Inertia effects are neglected as the frequency ω is sufficiently small, i.e.

$\omega \ll \frac{1}{L^2} \sqrt{\frac{EI_z}{\rho S}}$ where E is the Young modulus, ρ the volumic mass, I_z the quadratic moment of the cross-section about the z -axis and S the cross-sectional area (see CHRISTENSEN [2]).

Under the assumption of pure bending and small deformation, each material element is under uniaxial stress state $\sigma_{xx}(y, t)$ (other $\sigma_{ij} = 0$).

As the temperature variation is small during a cycle, the temperature distribution appears in the first approximation as an even function of the coordinate y : $T_m(y, t) = T_m(-y, t)$. The material presents the same response in tension and in compression and consequently, the uniaxial stress state is an odd function of the coordinate y : $\sigma_{xx}(y, t) = -\sigma_{xx}(-y, t)$. The deviatoric stresses and the hydrostatic pressure are also odd functions of the coordinate y : $s_{ij}(y, t) = -s_{ij}(-y, t)$ and $p(y, t) = -p(-y, t)$. As the radial stresses (σ_{yy}, σ_{zz}) are assumed to be negligible in pure bending, the stress decomposition (2.4) induces $s_{yy} = s_{zz} = p(y, t)$.

The usual development under small deformation assumption leads to the following expression for the axial strain ε_{xx} at the coordinate y at the time t :

$$\varepsilon_{xx}(y, t) = \frac{y}{L} \Theta(t).$$

Using the prescribed kinematic assumption (2.2), the axial strain is expressed as:

$$(2.6) \quad \varepsilon_{xx}(y, t) = \frac{y}{e} (\varepsilon_m + \varepsilon_0 \sin \omega t)$$

with $\varepsilon_m = \frac{e\Theta_m}{L}$ and $\varepsilon_0 = \frac{e\Theta_0}{L}$.

The deviatoric stresses are expressed after substitution into the Boltzmann law (2.5). As $\varepsilon_{ii} = 0$ due incompressibility, we obtain $\varepsilon_{yy} = \varepsilon_{zz} = -\varepsilon_{xx}/2$. It yields $s_{yy} = s_{zz} = -s_{xx}/2 = p(y, t)$. The axial stress has the form:

$$(2.7) \quad \sigma_{xx} = (3/2)s_{xx}.$$

2.2. Visco-elastic behavior in cyclic loading

The amplitude of temperature oscillations resulting from the sinusoidal solicitation is small enough to substitute in the constitutive law the temperature averaged over a cycle $T_m = \omega/2\pi \int_{t_0}^{t_0+2\pi/\omega} T(t)dt$ in place of the temperature T .

After substitution of the strain tensor (2.6) into the constitutive law (2.5), it follows that:

$$(2.8) \quad s_{xx} = 2G_\infty(T_m) \varepsilon_m \frac{y}{e} + 2\varepsilon_0 [G'(\omega, T_m) \sin \omega t + G''(\omega, T_m) \cos \omega t] \frac{y}{e}$$

where ε_m is the strain response to the static loading Θ_m . The frequency and temperature-dependent storage and loss moduli, $G'(\omega, T_m)$ and $G''(\omega, T_m)$ given by

$$G'(\omega, T_m) = G_\infty(T_m) + \omega \int_0^\infty (G(u, T_m) - G_\infty(T_m)) \sin(\omega u) du,$$

$$G''(\omega, T_m) = \omega \int_0^\infty (G(u, T_m) - G_\infty(T_m)) \cos(\omega u) du,$$

are proportional respectively to the average stored energy and dissipated energy in a cycle.

MOLINARI and GERMAIN [12] conducted the tests for different frequencies and various temperatures on a Pebax elastomer and have demonstrated the existence of master curves describing the storage and loss moduli in the range of tests. Similarly, we describe the variations of the moduli in terms of the reduced temperature $T_r = T - (1/\beta) \ln(\omega/\omega_0)$, where β and ω_0 are material characteristics:

$$(2.9) \quad G'(\omega, T) = h_1 - h_2 T_r,$$

$$(2.10) \quad G''(\omega, T) = g_1 - g_2 T_r = g_2 (T_\omega - T).$$

The frequency-dependent temperature T_ω is introduced for the sake of simplicity:

$$(2.11) \quad T_\omega = \frac{g_1}{g_2} + \frac{1}{\beta} \ln(\omega/\omega_0).$$

The material parameters describing the behavior of a Pebax elastomer are given in Sec. 4.

2.3. Heat equation

The evolution of the temperature is assumed to be governed by the linear heat equation using the assumption of transverse heat transfer:

$$(2.12) \quad \rho c \frac{\partial T}{\partial t} - k \frac{\partial^2 T}{\partial y^2} = \dot{Q},$$

where ρ is the density, c the specific heat capacity, k the heat conductivity and \dot{Q} the energy dissipated per unit time and unit volume.

Under steady state conditions, the heat generated through dissipation over a cycle is balanced by the heat loss into the surroundings. The averaged temperature T_m over a cycle is time-independent. The spatial distribution of the averaged temperature T_m satisfies the heat equation (2.12) averaged over a cycle:

$$(2.13) \quad -k \frac{d^2 T_m}{dy^2} = \frac{\omega}{2\pi} \Delta Q^{st} = \overline{\Delta Q}^{st},$$

where $\overline{\Delta Q}^{st}$ is the time average per cycle of the energy dissipated per unit volume:

$$(2.14) \quad \overline{\Delta Q}^{st} = \frac{\omega}{2\pi} \int_0^{2\pi/\omega} \dot{Q}(t) dt.$$

Since the dissipated energy per cycle is given by the hysteresis loop, we have:

$$(2.15) \quad \overline{\Delta Q}^{st} = \frac{\omega}{2\pi} \int_0^{2\pi/\omega} \sigma_{ij} \dot{\epsilon}_{ij} dt.$$

Thermal dilatation is not taken into account in the following analysis. The end faces A and B (Fig. 1a) are assumed to be adiabatic. The temperature distribution appears also as an even function of the variable y . The thermal boundary conditions specify the heat transfer at the lateral boundaries $y = e$ and vanishing of the heat flux along the neutral axis $y = 0$:

$$(2.16) \quad k \frac{dT_m}{dy} + \lambda (T_m - T_0) = 0 \quad \text{at} \quad y = e,$$

$$(2.17) \quad k \frac{dT_m}{dy} = 0 \quad \text{at} \quad y = 0,$$

where λ is the heat transfer coefficient at the external boundary and T_0 is the external temperature.

3. Steady state response

The steady state response is analyzed first; in that case, the heat generated by dissipation during a cycle is exactly balanced by the heat transferred to the surroundings.

3.1. Temperature distribution

The dissipated energy is evaluated from Eq. (2.15):

$$(3.1) \quad \overline{\Delta Q}^{st} = \frac{3}{2} \frac{\omega}{e^2} \varepsilon_0^2 y^2 G''(\omega, T_m),$$

where the dissipation modulus is expressed by Eq. (2.10). As a consequence of (2.13), the average temperature satisfies the differential equation

$$(3.2) \quad \frac{d^2 T_m}{dy^2} - a^2 y^2 T_m = -a^2 y^2 T_\omega,$$

$$(3.3) \quad \text{with } a^2 = \frac{3}{2k} \frac{\omega}{e^2} g_2 \varepsilon_0^2.$$

The temperature distribution T_m involves the modified Bessel functions $I_{1/4}$ and $I_{-1/4}$ (WATSON [23]):

$$(3.4) \quad T_m(y) = T_\omega + \kappa_1 \sqrt{y} I_{-1/4}(ay^2/2) + \kappa_2 \sqrt{y} I_{1/4}(ay^2/2),$$

with (κ_1, κ_2) determined so as to satisfy the thermal boundary conditions (2.16) and (2.17). As the derivative of the function $\sqrt{y} I_{-1/4}(ay^2/2)$ versus y is $\frac{a}{2} y^{3/2} I_{3/4}(ay^2/2)$ and vanishes for $y = 0$, it can be shown using Eq. (2.17) that $\kappa_2 = 0$. Taking account of the thermal boundary condition at $y = e$ (2.16), the temperature distribution reads:

$$(3.5) \quad T_m(y) = T_\omega + \kappa_1 \sqrt{y} I_{-1/4}(ay^2/2)$$

with

$$(3.6) \quad \kappa_1 = \frac{\lambda(T_0 - T_\omega)}{[kae^{3/2} I_{3/4}(ae^2/2) + \lambda\sqrt{e} I_{-1/4}(ae^2/2)]}.$$

3.2. Resulting bending moment

In some experiments, a prescribed bending moment is transmitted to the specimen at the end face B , the end face A remaining fixed. The relation between the amplitude of the bending moment and the axial deformation has to

be established. The phase angle between the applied curvature and the resulting moment derives from the dissipative effects. In case of uniform temperature distribution, the phase angle is identical to the loss tangent defined as $\tan \psi = \frac{G''(\omega, T_m)}{G'(\omega, T_m)}$.

The bending moment is calculated in terms of stress by $M(t) = 2l \int_{-e}^e \sigma_{xx} y dy = 3l \int_{-e}^e s_{xx} y dy$ which can be transformed to:

$$(3.7) \quad M = M_m + M_1 \sin \omega t + M_2 \cos \omega t = M_m + M_0 \sin(\omega t + \varphi),$$

where

$$(3.8) \quad M_m = 12 \frac{l}{e} \varepsilon_m \int_0^e G_\infty(T_m(y)) y^2 dy,$$

$$(3.9) \quad M_0 = \sqrt{M_1^2 + M_2^2},$$

$$(3.10) \quad \tan \varphi = M_2/M_1,$$

$$(3.11) \quad M_1 = 12 \frac{l}{e} \varepsilon_0 \int_0^e G'(\omega, T_m) y^2 dy,$$

$$M_2 = 12 \frac{l}{e} \varepsilon_0 \int_0^e G''(\omega, T_m) y^2 dy.$$

Using (3.5), we have:

$$(3.12) \quad M_1 = 4le^2 \varepsilon_0 h_2 \left[\left(\frac{h_1}{h_2} - \frac{g_1}{g_2} \right) - 3\kappa_1 \frac{1}{ae^{3/2}} I_{3/4}(ae^2/2) \right]$$

$$(3.13) \quad M_2 = -12 \frac{l}{a} e^{1/2} \varepsilon_0 g_2 \kappa_1 I_{3/4}(ae^2/2).$$

4. Parametric analysis

The cross-section of the beam drawn in Fig. 1a is defined by its half-height $e = 5 \cdot 10^{-3}$ m and its half-width $l = 25 \cdot 10^{-3}$ m. The parametric analysis is conducted at the reference temperature $T_0 = 320$ K. The influence of the loading parameters is described in terms of deformation amplitude, bending moment

and pulsation frequency. Effects of the geometry are studied in connection with their contribution to the heat diffusion process. The material considered here is a thermoplastic elastomer, where the amorphous polyether phase is crosslinked by a semi-crystalline polyamid (PEBA). The material tests for characterising the storage and loss moduli $G'(\omega, T)$ (2.9) and $G''(\omega, T)$ (2.10) are conducted at different frequencies and various temperatures. The results can be synthetised on a single master curve (FERRY [4]). The melting temperature is 441 K. The mechanical and thermal properties are presented by MOLINARI and GERMAIN [12] in the following table for a Peba of Shore D and hardness 40.

The coefficients h_1 , h_2 , g_1 and g_2 are constant in the temperature interval $T_r > 314$ K.

Peba		Material parameters	
	MPa	ω_0	628 rad/s
h_1	91	β	0.4 K ⁻¹
h_2	0.193	k	0.2 Wm ⁻¹ K ⁻¹
g_1	3.1	λ	20 Wm ⁻² K ⁻¹
g_2	0.006	ρc	2 10 ⁶ Wm ⁻³ K ⁻¹

4.1. The influence of the loading parameters

The evolution of the mean temperature T_m for increasing deformation is represented in terms of the deformation ε_0 in Fig. 2 for $\omega = 50$ rad/s and for $\varepsilon_m = 0$. The largest temperature is observed at the specimen center where the heat diffusion towards the surroundings is limited.

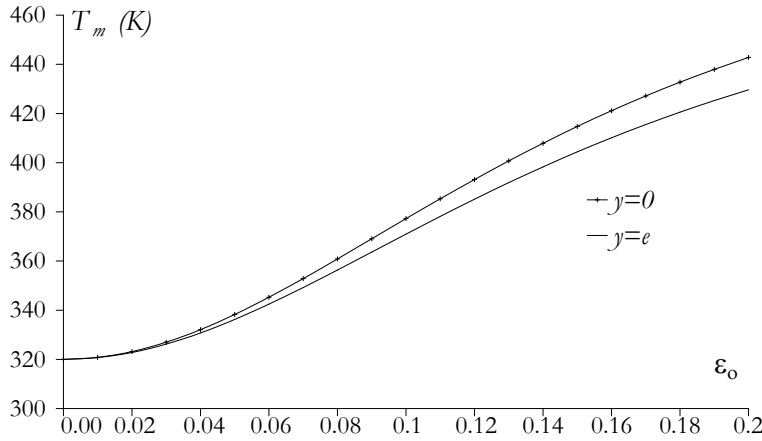


FIG. 2. Temperature at the center $y = 0$ and at the lateral boundary $y = e$ with respect to $\varepsilon_0 = \frac{e\Theta_0}{L}$ (for $\omega = 50$ rad/s).

For a given frequency, we have $M_m = 0$ and the bending moment M_0 (calculated from Eqs. (3.9) with (3.12) and (3.13)) presents an extremum M_0^{cr} at a critical value ε_0^{cr} (Fig. 3). Two types of loading conditions are analyzed: a prescribed curvature (2.2) or a prescribed moment (2.3). Under the cyclic kinematic $\varepsilon_m = 0$, when the deformation amplitude $\varepsilon_0 = e\Theta_0/L$ and the frequency ω are imposed, only one bending moment M_0 is associated to steady state regime. For a bending moment M_0 larger than M_0^{cr} , the solution presented in Fig. 3 shows that no steady state regime can be established. When the prescribed bending moment M_0 is smaller than M_0^{cr} , two steady-state regimes can be described provided that the melting temperature is not reached. The stability of the regimes is analyzed in the next section.

Alternatively, the bending moment M_0 may be analysed in terms of frequency ω when the deformation ε_0 is fixed (Fig. 4). The thermal softening effects are amplified at high frequency regime since the dissipated energy is less evacuated to the surroundings. For larger values of ε_0 , the frequency associated with the extremum of bending decreases.

The critical deformation ε_0^{cr} defined before decreases when the frequency increases (Fig. 5). As a consequence, for an assumed value of the moment M_0 , the steady-state solution becomes unstable when the frequency ω reaches a critical value. For instance, in Fig. 5, the critical value of ω is $100 \text{ rad} \cdot \text{s}^{-1}$ for $M_0 = 3 \text{ Nm}$. SCHAPERY and CANTEY [17] have already discussed in their Figure 10 the existence of this type of instability.

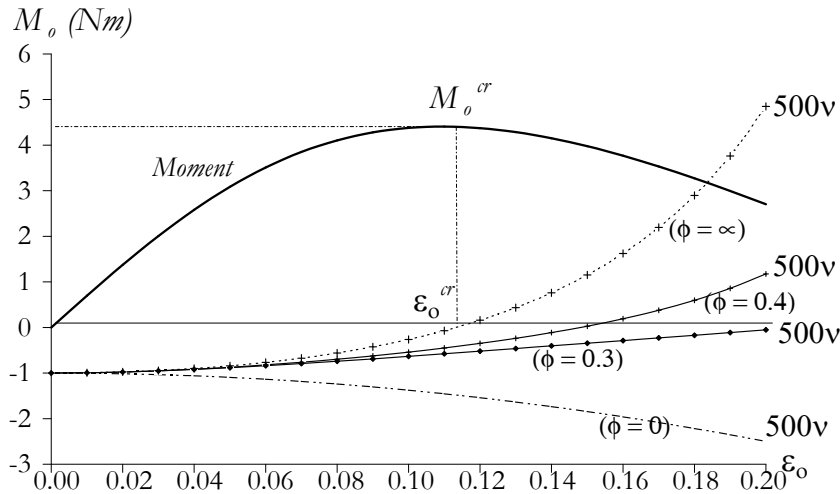


FIG. 3. Evolution of the bending moment M_0 in terms of $\varepsilon_0 = e\Theta_0/L$ (for $\omega = 50 \text{ rad/s}$). Note the evolution of the rate of growth ν as a function of the boundary conditions. The neutral stability point defined by $\nu = 0$ under prescribed moment ($\phi \rightarrow \infty$) corresponds to the maximum of the M_0 versus the ε_0 curve. The ascending branch is stable ($\nu < 0$) and the descending branch ($\nu > 0$) are unstable.

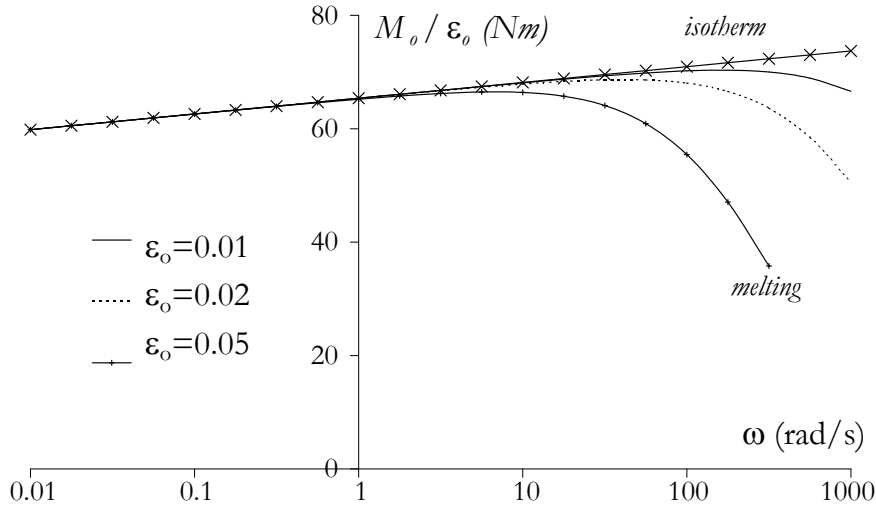


FIG. 4. Evolution of the bending moment in terms of the frequency ω .

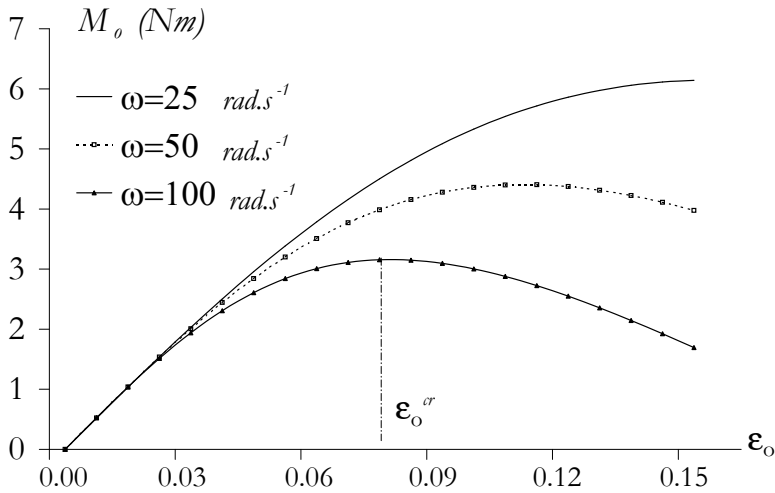


FIG. 5. Amplification of the thermal effects with larger values of the frequency ω .

The axial stress profile defined by $\sigma_0(y) = 3\varepsilon_0 \frac{y}{e} \sqrt{G'(\omega, T_m)^2 + G''(\omega, T_m)^2}$ for $\varepsilon_m = 0$ is analyzed for two deformation amplitudes ε_0 in Fig. 6. The bending moment M_0 can be related to an equivalent axial stress σ_{0e} introduced when a linear stress distribution of the form $\sigma_{0e}(y) = \frac{y}{e} \sigma_{0e}$ is considered: $M(t) = 2l \int_{-e}^e \frac{\sigma_{0e}}{e} y^2 dy = \frac{\sigma_{0e}}{e} I_z$, where $I_z = 4le^3/3$ is the quadratic moment of the

cross-section area about the z -axis. Figure 6 shows that the axial stress profile $\sigma_0(y)$ differs from the equivalent stress profile $\sigma_{0e}(y)$ when the amplitude of the deformation ε_0 increases: the boundary layers of the beam appear more constrained.

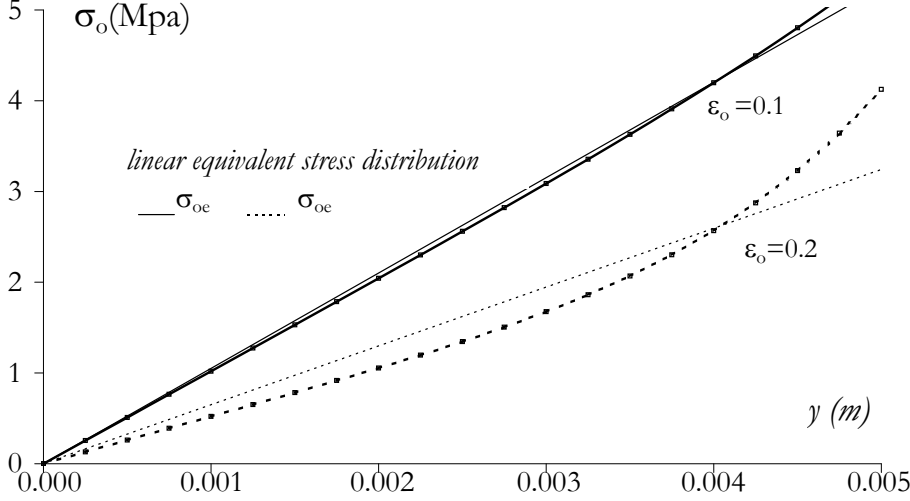


FIG. 6. Axial stress profiles at two values of $\varepsilon_0 = e\Theta_0/L$.

4.2. Effects of the geometry

The maximum axial stress at the lateral boundary $\sigma_0(e) = 3\varepsilon_0 \sqrt{G'(\omega, T_m)^2 + G''(\omega, T_m)^2}$ is plotted in Fig. 7 versus the amplitude deformation for various widths. For increasing width, the maximum amplitude of the axial stress at the boundary $\sigma_0^{\text{cr}}(e)$ and the corresponding critical amplitude deformation $\varepsilon_0^{\text{cr}}$ decrease.

Let us consider the first-order expansion of the modified Bessel functions $I_{-1/4}$ (WATSON [23]): $I_{-1/4}(ay^2/2) = \sqrt{2} \frac{a^{-1/4}}{\Gamma(3/4)} y^{-1/2}$. The first-order asymptotic expansion of the temperature distribution (3.5) with respect to ay^2 for both loading modes has the form:

$$(4.1) \quad T_m(y) = T_\omega + \frac{T_0 - T_\omega}{\left(\frac{\omega g_2 e}{2\lambda} \varepsilon_0^2 + 1\right)} + o(ay^2).$$

At the first order, the temperature distribution does not depend on the variable y .

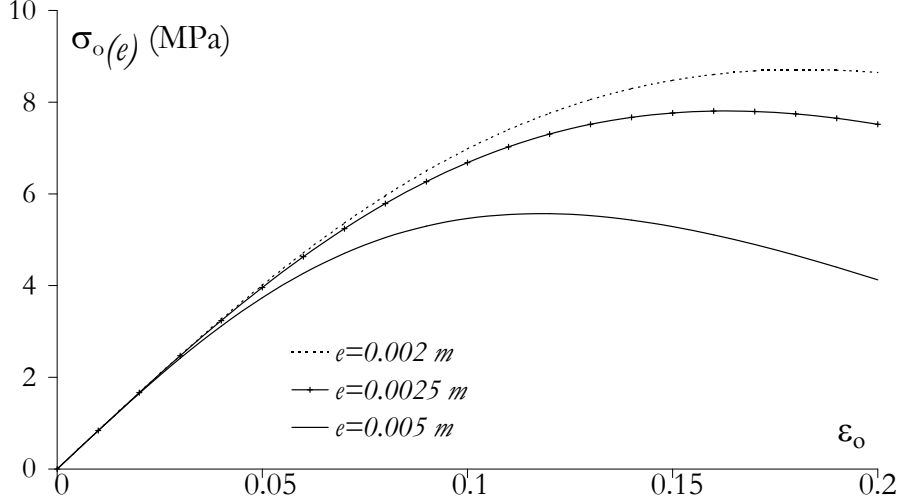


FIG. 7. Evolution of the amplitude $\sigma_0(e)$ of the axial stress at the boundary versus $\varepsilon_0 = \frac{e\Theta_0}{L}$.

The bending moment M_0 is also approached by its expansion versus ay^2 at the first order:

$$(4.2) \quad M_0 = 4le^2\varepsilon_0g_2(T_\omega - T_m) \left[1 + \left(\frac{h_2}{g_2} \right)^2 \left[1 + \frac{1}{(T_m - T_\omega)} \left(\frac{h_1}{h_2} - \frac{g_1}{g_2} \right) \right]^2 \right]^{1/2} + o(ay^2)$$

with $T_m = T_\omega + \frac{T_0 - T_\omega}{\left(\frac{\omega g_2 e}{2\lambda} \varepsilon_0^2 + 1 \right)}$. The contribution of the heat transfer coefficient

λ at the external boundary may be analyzed in connection with the width influence. When the ratio λ/e is kept constant, the temperature (4.1) is unchanged while the bending moment (4.2) is multiplied by a factor κ^2 when the width e is changed by κe (Fig. 8). As a consequence, the amplitude of the critical bending moment M_0^{cr} corresponds to the same critical deformation amplitude $\varepsilon_0^{\text{cr}}$ and critical temperature T_m^{cr} for a constant ratio λ/e .

5. Linear stability analysis

So far, the analysis has been restricted to the mathematical existence of the steady-state solutions, but their physical existence, which depends on their

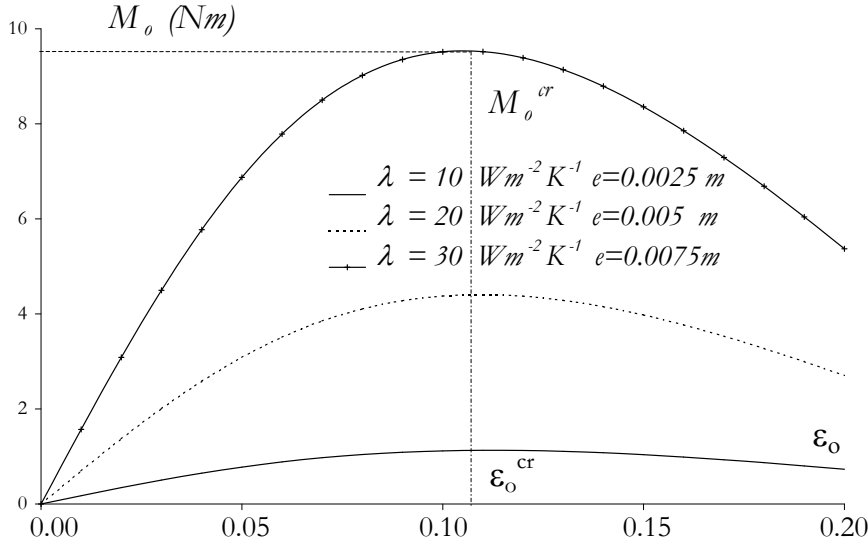


FIG. 8. Effect of the heat transfer coefficient λ on steady states.

stability, was not established. This section is aimed at analysing the influence of the loading conditions on the stability of steady states.

5.1. Preliminary consideration to the linearized stability analysis

We consider weak instabilities for which the characteristic time of growth is large with respect to the period of a cycle. The temperature evolution is described using two time-scales:

- the fast time $t_0 = t$ describes the variations of temperature, stress and strain in a cycle,
- the slow time $t_1 = \epsilon t$ – with ϵ being small parameter – follows the development of the instability throughout the successive cycles. The average temperature \bar{T} over a cycle is defined as

$$(5.1) \quad \bar{T}(y, t_1) = \frac{\omega}{2\pi} \int_{t_0}^{t_0+2\pi/\omega} T(y, t'_0, t_1) dt'_0.$$

The time-dependence of \bar{T} is slow since the evolution of the averaged temperature is controlled by the weak instability. The stability of the steady state solution is inferred by considering a small perturbation of the stationary temperature profile $T_m(y)$ and looking on the evolution of the average temperature $\bar{T}(y, t_1)$ at times much larger than the period $2\pi/\omega$. Time averaging in a cycle

of the heat equation (2.12) leads to:

$$(5.2) \quad \rho c \frac{\partial \bar{T}}{\partial t} - k \frac{\partial^2 \bar{T}}{\partial y^2} = \overline{\Delta Q}.$$

To demonstrate (5.2), we have used the following relationships:

$$\frac{\partial}{\partial t} T(y, t_0, t_1) = \frac{\partial T}{\partial t_0} + \epsilon \frac{\partial T}{\partial t_1}$$

and

$$\frac{\partial \bar{T}}{\partial t} = \epsilon \frac{\partial \bar{T}}{\partial t_1} = \epsilon \frac{\partial \bar{T}}{\partial t_1} = \frac{\partial \bar{T}}{\partial t}$$

(expressions developed by MOLINARI and GERMAIN [12]). The energy dissipated per unit volume and per cycle at the time t is expressed as:

$$(5.3) \quad \overline{\Delta Q} = \frac{\omega}{2\pi} \int_{t_0}^{t_0+2\pi/\omega} \sigma_{ij}(y, t'_0, t_1) \dot{\epsilon}_{ij}(y, t'_0, t_1) dt'_0$$

and is considered as the superimposition of a perturbation to the heat generated in stable regime:

$$(5.4) \quad \overline{\Delta Q} = \overline{\Delta Q}^{st} + \Delta \hat{Q} \exp \nu t$$

with $\overline{\Delta Q}^{st}$ given by (3.1). The average temperature is considered as the superimposition of a perturbation $\delta \bar{T}(y, t)$ to the steady temperature $T_m(y)$:

$$(5.5) \quad \bar{T}(y, t) = T_m(y) + \delta \bar{T}(y, t) = T_m(y) + \delta \hat{T}(y) \exp \nu t.$$

The perturbation is supposed to be separated into space and time contributions, where ν denotes the rate of growth of the perturbation. The steady state solution is linearly stable if the real part of ν is negative. After subtraction of (2.13) from (5.2), a differential equation governing the perturbation $\delta \hat{T}(y)$ is obtained:

$$(5.6) \quad \nu \left(\frac{\rho c}{k} \delta \hat{T}(y) \right) - \frac{d^2 \delta \hat{T}(y)}{dy^2} = \frac{1}{k} \Delta \hat{Q},$$

where the expression $\Delta \hat{Q}$ is determined as the local increase of energy dissipated per cycle. When instability occurs, the amplitude of the response varies with time. We define the amplitude of the axial strain by ε_a and a similar decomposition as for the temperature perturbation (5.5) is considered (see Appendix A):

$$(5.7) \quad \varepsilon_a = \varepsilon_0 + \delta \bar{\varepsilon}(t) = \varepsilon_0 + \delta \hat{\varepsilon} \exp \nu t.$$

Note that ε_{xx} is given by (2.6) where ε_0 is replaced by ε_a . The bending moment given by $M(t) = M_m + M_a \sin \omega t$ with M_a decomposed into:

$$(5.8) \quad M_a = M_0 + \delta \bar{M}(t) = M_0 + \delta \hat{M} \exp \nu t.$$

The increment of energy dissipated per cycle can be expressed as a function of deformation and temperature increment (see Appendix A):

$$(5.9) \quad \frac{1}{k} \Delta \hat{Q} = a^2 y^2 \left[2 \frac{\delta \hat{\varepsilon}}{\varepsilon_0} (T_\omega - T_m(y)) - \delta \hat{T} \right].$$

The temperature perturbation $\delta \hat{T}(y)$ has also to satisfy the thermal boundary conditions and the symmetry condition at $y = 0$:

$$(5.10) \quad k \frac{d\delta \hat{T}(y)}{dy} + \lambda \delta \hat{T}(y) = 0 \quad \text{at } y = e,$$

$$(5.11) \quad k \frac{d\delta \hat{T}(0)}{dy} = 0.$$

5.2. Stability analysis for a prescribed curvature

Prescribed deformation imposes $\delta \hat{\varepsilon} = 0$. From Eqs. (5.6) and (5.9), it follows that the temperature perturbation satisfies the differential equation:

$$(5.12) \quad \nu \left(\frac{\rho c}{k} \delta \hat{T}(y) \right) - \frac{d^2 \delta \hat{T}(y)}{dy^2} = -a^2 y^2 \delta \hat{T}(y).$$

The conditions of neutral stability $\nu = 0$ corresponds to vanishing of the rate of growth of the perturbation. It is seen that $\delta \hat{T}(y)$ satisfies the same type of equation as the homogeneous part of the Eq. (3.2) governing the steady state temperature T_m . The solution is expressed as $\delta \hat{T}(y) = \chi_1 \sqrt{y} I_{-1/4}(ay^2/2) + \chi_2 \sqrt{y} I_{1/4}(ay^2/2)$, where the constants (χ_1, χ_2) are determined by the thermal boundary conditions (5.10) and (5.11). It is numerically observed that no values different from $(\chi_1 = 0, \chi_2 = 0)$ can be found to satisfy the condition of neutral stability $\nu = 0$. Therefore, the sign of ν is determined by considering a particular loading, for instance a zero amplitude of strain. Then the evolution of $\delta \hat{T}(y)$ satisfies the equation: $\nu \left(\frac{\rho c}{k} \delta \hat{T}(y) \right) - \frac{d^2 \delta \hat{T}(y)}{dy^2} = 0$. This equation and the associated thermal boundary conditions are similar to those analyzed by LEROY and MOLINARI [13]. These authors have shown that $\nu < 0$. Consequently, the steady state solutions under prescribed curvature are stable.

5.3. Stability analysis for a prescribed bending moment

The amplitude M_a of the bending moment is given by $M_a = \sqrt{M_1^2 + M_2^2}$ with M_1 and M_2 obtained from (3.11), where ε_0 is replaced by ε_a and T_m by \bar{T} . The substitution is valid when weak instabilities are considered. Then $\delta\hat{M}$ is derived from (5.8) (see Appendix B). For a prescribed moment, $\delta\hat{M} = 0$. A combined linearisation of ε_a and \bar{T} at the first order gives the following relationship:

$$(5.13) \quad \frac{\delta\varepsilon}{\varepsilon_0} = \frac{\left[\int_0^e (h_2 G'(\omega, T_m) + g_2 G''(\omega, T_m)) y^2 dy \right] \left[\int_0^e \delta\hat{T} y^2 dy \right]}{\left[\left(\int_0^e G'(\omega, T_m) y^2 dy \right)^2 + \left(\int_0^e G''(\omega, T_m) y^2 dy \right)^2 \right]}.$$

Using (5.6) and (5.9), the temperature perturbation satisfies the differential equation:

$$(5.14) \quad \nu \left(\frac{\rho c}{k} \delta\hat{T}(y) \right) - \frac{d^2 \delta\hat{T}(y)}{dy^2} \\ = a^2 y^2 \left[2 \frac{\left[\int_0^e (h_2 G'(\omega, T_m) + g_2 G''(\omega, T_m)) y^2 dy \right] \left[\int_0^e \delta\hat{T}(y) y^2 dy \right]}{\left[\left(\int_0^e G'(\omega, T_m) y^2 dy \right)^2 + \left(\int_0^e G''(\omega, T_m) y^2 dy \right)^2 \right]} \right. \\ \left. \cdot (T_\omega - T_m(y)) - \delta\hat{T}(y) \right].$$

The critical steady state corresponds to neutral stability ($\nu = 0$) and is obtained for the value $\varepsilon_0^{\text{cr}}$ of the amplitude. No closed-form solution is available for the integro-differential equations (5.14) with $\nu = 0$. However, by using the Bubnov–Galerkin method, one could give, as in DINZART and MOLINARI [3], an estimation of the critical axial strain $\varepsilon_0^{\text{cr}}$. The amplitude of the perturbation $\delta\hat{T}(y)$ is expressed as a linear combination of basis quadratic functions ($\Phi_1 = a_1 + b_1 y - y^2$, $\Phi_2 = a_2 + b_2 y^3 - y^4$) such that $\delta\hat{T}(y) = c_1 \Phi_1(y) + c_2 \Phi_2(y)$. The constants (a_1, b_1, a_2, b_2) are determined in order to satisfy the thermal boundary conditions. The orthogonality conditions written for the residuals of the differential equation (5.14) provide a linear system for (c_1, c_2). Setting the determinant of this system equal to zero provides the critical amplitude $\varepsilon_0^{\text{cr}}$ of the steady state corresponding to the neutral state. It can be shown that steady states of amplitude ε_0 are stable for $\varepsilon_0^{\text{cr}} > \varepsilon_0$ and unstable for $\varepsilon_0^{\text{cr}} < \varepsilon_0$.

5.4. Assumption of temperature uniformity in a cross-section

Simple stability results are obtained when some simplifying assumptions are made. When the specimen is thin enough, the temperature within a cross-section can be assumed as quasi-uniform. Then, explicit results are obtained concerning the critical strains $\varepsilon_0^{\text{cr}}$ and the corresponding values of the moment M_0^{cr} . The energy equation (2.12) is first averaged over the thickness of the sample¹⁾:

$$(5.15) \quad \rho c \left\langle \frac{\partial T(y, t)}{\partial t} \right\rangle - k \left\langle \frac{\partial^2 T(y, t)}{\partial y^2} \right\rangle = \langle \dot{Q} \rangle,$$

where $k \left\langle \frac{\partial^2 T(y, t)}{\partial y^2} \right\rangle$ is simplified to $\frac{\lambda}{e} (T(t) - T_0)$ when considering thermal boundary conditions. The resulting energy equation is averaged over a cycle in view to determine the mean temperature evolution:

$$(5.16) \quad \rho c \frac{d\bar{T}(t)}{dt} + \frac{\lambda}{e} (\bar{T}(t) - T_0) = \langle \overline{\Delta Q} \rangle,$$

where $\langle \overline{\Delta Q} \rangle$ is defined from the space averaging of the energy dissipated per unit volume and per cycle by (5.3). The perturbed temperature $\bar{T}(t)$ is expressed as the superposition of the steady temperature T_m and a small perturbation $\delta\bar{T}(t)$. Instability is related to the growth of $\delta\bar{T}(t)$ with time. It is seen that the steady temperature T_m satisfies the equation derived from (5.16) (see Appendix C):

$$(5.17) \quad \frac{\lambda}{e} (T_m - T_0) = \langle \overline{\Delta Q}^{\text{st}} \rangle = \frac{ke^2 a^2}{3} (T_\omega - T_m).$$

Then the mean temperature is written as:

$$(5.18) \quad T_m = \frac{a^2 + \frac{3\lambda}{ke^3} \frac{T_0}{T_\omega}}{a^2 + \frac{3\lambda}{ke^3}} T_\omega = \frac{\frac{\omega g_2 e}{2\lambda} \varepsilon_0^2 + \frac{T_0}{T_\omega}}{\frac{\omega g_2 e}{2\lambda} \varepsilon_0^2 + 1} T_\omega.$$

The evolution of the perturbation $\delta\bar{T}(t)$ is obtained as the difference of Eqs. (5.17) and (5.16):

$$(5.19) \quad \rho c \frac{d\delta\bar{T}(t)}{dt} + \frac{\lambda}{e} \delta\bar{T}(t) = \langle \overline{\Delta Q} \rangle - \langle \overline{\Delta Q}^{\text{st}} \rangle.$$

¹⁾The notation " $\langle \rangle$ " corresponds to spatial averaging in a cross-section: $\langle f(y, t) \rangle = \frac{1}{2e} \int_{-e}^e f(y, t) dy$.

The axial strain and bending moment amplitudes are expressed as a function of the mean temperature over a cycle:

$$(5.20) \quad \varepsilon_a(\bar{T}(t)) = \varepsilon_0(T_m) + \delta\bar{\varepsilon}(\delta\bar{T}(t)),$$

$$(5.21) \quad M_a(\bar{T}(t)) = M_0(T_m) + \delta\bar{M}(\delta\bar{T}(t)).$$

The energy increase $\langle\overline{\Delta Q}\rangle - \langle\overline{\Delta Q}^{st}\rangle$ is evaluated in Appendix C:

$$(5.22) \quad \left(\langle\overline{\Delta Q}\rangle - \langle\overline{\Delta Q}^{st}\rangle\right) = \frac{ke^2a^2}{3} \left[2\frac{\delta\bar{\varepsilon}(\delta\bar{T}(t))}{\varepsilon_0}(T_\omega - T_m) - \delta\bar{T}\right].$$

By inserting (5.19) into (5.22), the energy equation takes the following form:

$$(5.23) \quad \rho c \frac{d\delta\bar{T}(t)}{dt} + \frac{\lambda}{e}\delta\bar{T}(t) = \frac{ke^2a^2}{3} \left[2\frac{\delta\bar{\varepsilon}(\delta\bar{T}(t))}{\varepsilon_0}(T_\omega - T_m) - \delta\bar{T}\right].$$

The linear dependence of $\delta\bar{\varepsilon}$ upon $\delta\bar{T}$ will be expressed later. The growth rate ν of the perturbation, as defined by (5.5), follows the Eq. (5.24) according to (5.23).

$$(5.24) \quad \frac{d\delta\bar{T}(t)}{dt} - \nu\delta\bar{T}(t) = 0.$$

5.4.1. Prescribed curvature. For kinematically controlled boundary conditions, we have $\delta\bar{\varepsilon} = 0$. The evolution of the perturbation $\delta\bar{T}(t)$ is governed by:

$$\rho c \frac{d\delta\bar{T}(t)}{dt} + \frac{\lambda}{e}\delta\bar{T}(t) = -\frac{ke^2a^2}{3}\delta\bar{T}$$

with $a^2 = \frac{3}{2k} \frac{\omega}{e^2} g_2 \varepsilon_0^2$. As a consequence, the rate of growth is expressed as:

$$\nu_\varepsilon = -\frac{1}{\rho c} \left(\frac{\omega g_2 \varepsilon_0^2}{2} + \frac{\lambda}{e} \right).$$

Since ν_ε is negative, all steady states are stable for kinematically controlled boundary conditions.

5.4.2. Prescribed bending moment. For prescribed bending, the strain amplitude perturbation is expressed as in Sec. 5.3 and simplified under the hypothesis of uniform temperature distribution in a cross-section:

$$(5.25) \quad \frac{\delta\bar{\varepsilon}}{\varepsilon_0} = -\mathbb{G}(T_m)\delta\bar{T},$$

with $\mathbb{G}(T_m) = \left(\frac{\frac{dG'}{dT}G' + \frac{dG''}{dT}G''}{G' + G''} \right) (T_m)$. After substitution of this expression into (5.23), the rate of growth of the perturbation is expressed as:

$$(5.26) \quad \nu_M = -\frac{1}{\rho c} \left(\frac{\omega g_2 \varepsilon_0^2}{2} (2\mathbb{G}(T_m)(T_\omega - T_m) + 1) + \frac{\lambda}{e} \right).$$

The critical temperature T_m^{cr} at the stability transition satisfies $\nu_M = 0$. By using Eqs. (3.3) and (5.17), this condition can be written as:

$$(5.27) \quad 1 + \frac{(T_m^{\text{cr}} - T_0)}{(T_\omega - T_m^{\text{cr}})} (2\mathbb{G}(T_m^{\text{cr}})(T_\omega - T_m^{\text{cr}}) + 1) = 0.$$

It is worth noting that T_m^{cr} depends on the external temperature T_0 and the pulsation frequency.

The corresponding strain amplitude is given by substituting (5.27) in (5.26) with $\nu_M = 0$, or by using (5.18):

$$(5.28) \quad \varepsilon_0^{\text{cr}^2} = \frac{2\lambda}{e\omega g_2} \frac{(T_m^{\text{cr}} - T_0)}{(T_\omega - T_m^{\text{cr}})}$$

and the critical bending moment is obtained after substitution into (3.9) and (3.11). Under the assumption of temperature uniformity, it follows that:

$$(5.29) \quad M_0^{\text{cr}} = \frac{8\lambda l e}{\omega \varepsilon_0^{\text{cr}}} (T_m^{\text{cr}} - T_0) \left[1 + \left(\frac{h_2}{g_2} \right)^2 \left[1 + \frac{1}{(T_\omega - T_m^{\text{cr}})} \left(\frac{h_1}{h_2} - \frac{g_1}{g_2} \right) \right]^2 \right]^{1/2}.$$

For a cyclic solicitation conducted at the frequency $\omega = 50$ rad/s and the room temperature $T_0 = 320$ K, the critical temperature is $T_m^{\text{cr}} = 381.78$ K for the Pebax elastomer. The corresponding strain amplitude and bending moment are: $\varepsilon_0^{\text{cr}} = 0.113$ and $M_0^{\text{cr}} = 4.559$ Nm.

5.4.3. Mixed mechanical boundary conditions. Mixed boundary conditions can be expressed as follows:

$$(5.30) \quad (\varepsilon_0 - \check{\varepsilon}) - \phi (M_0 - \check{M}) = 0,$$

where $\check{\varepsilon}$, \check{M} and $\phi \leq 0$ characterise the loading conditions. The limiting cases $\phi = 0$ and $\phi = \infty$ correspond respectively to the prescribed curvature and the prescribed bending moment. The perturbation of the bending moment is

expressed as $\delta\bar{M} = M_0 \left[\frac{\delta\bar{\varepsilon}}{\varepsilon_0} + \mathbb{G}(T_m) \delta\bar{T} \right]$. The perturbation of the strain amplitude $\delta\bar{\varepsilon}$ must satisfy the prescribed boundary condition, thus $\delta\bar{\varepsilon} - \phi\delta\bar{M} = 0$:

$$(5.31) \quad \frac{\delta\bar{\varepsilon}}{\varepsilon_0} = \left(\frac{\varepsilon_0}{\check{\varepsilon} - \phi\check{M}} - 1 \right) \mathbb{G}(T_m) \delta\bar{T}.$$

The rate of growth of the perturbation is given by:

$$(5.32) \quad \nu_\phi = -\frac{1}{\rho c} \left(\frac{\omega g_2 \varepsilon_0^2}{2} \left(1 - 2 \left(\frac{\varepsilon_0}{\check{\varepsilon} - \phi\check{M}} - 1 \right) \mathbb{G}(T_m) (T_\omega - T_m) \right) + \frac{\lambda}{e} \right).$$

The critical temperature T_m^{cr} at the stability transition is a solution of the equation $\nu_\phi = 0$, which by using (3.3) and (5.17) is written in the form:

$$(5.33) \quad 1 + \frac{(T_m^{\text{cr}} - T_0)}{(T_\omega - T_m^{\text{cr}})} \left(1 - 2 \left(\frac{\varepsilon_0^{\text{cr}}}{\check{\varepsilon} - \phi\check{M}} - 1 \right) \mathbb{G}(T_m^{\text{cr}}) (T_\omega - T_m^{\text{cr}}) \right) = 0.$$

For a prescribed bending moment ($\phi = \infty$), the stability condition (5.27) is retrieved. The strain amplitude and the bending moment at the point of neutral stability are obtained as in the previous section by means of Eqs. (5.28) and (5.29).

Alternatively, for $\phi = 0$, we have from (5.30) $\check{\varepsilon} = \varepsilon_0$, and ν_ϕ given by (5.32) cannot vanish, therefore the stability is always insure for kinematically prescribed boundary condition.

Figure 3 shows that for a prescribed moment ($\phi = \infty$), the steady states at the neutral stability are unstable on the descending branch of the M_0 versus ε_0 curve. When the value of ϕ is decreased to zero, the range of stable steady state increases. For the value $\phi = 0$, all the steady states are stable.

6. Conclusion

The cyclic response of a rectangular beam made of viscoelastic material has been analyzed for pure cyclic bending. The behavior of the elastomer was assumed to be linear isotropic and incompressible. The loss and storage moduli following from the Boltzmann law were expressed as functions of the frequency and the temperature, thus inducing a thermomechanical coupling. The stress, strain and temperature fields were determined under stationary regime. The stability of these steady states has been analyzed by considering a weak perturbation in temperature, leading to a perturbation in the stress and strain fields. As already demonstrated in the case of compressive loading [12], a prescribed bending moment may initiate an unstable regime leading to a thermal runaway. When mixed boundary conditions are considered, stable and unstable regimes can also be defined.

Appendix A.

The perturbed temperature $\delta\bar{T}(t) = \bar{T} - T_m$ satisfies the differential equation following from the difference between Eq. (5.2) and the steady state heat Eq. (2.13):

$$(A.1) \quad \rho c \frac{\partial (\bar{T} - T_m)}{\partial t} - k \frac{\partial^2 (\bar{T} - T_m)}{\partial y^2} = \overline{\Delta Q} - \overline{\Delta Q}^{st},$$

which, if $\delta\bar{T}(y, t)$ is decomposed into space and time contribution, may be expressed as

$$(A.2) \quad \rho c \frac{\partial (\delta\hat{T}(y) \exp \nu t)}{\partial t} - k \frac{\partial^2 (\delta\hat{T}(y) \exp \nu t)}{\partial y^2} = \overline{\Delta Q} - \overline{\Delta Q}^{st}.$$

This operation is valid, because the instability process is supposed to be slow; therefore \bar{T} , ε_a and M_a can be considered as quasi-constant over several cycles.

From (3.1), we have $\overline{\Delta Q}^{st} = \frac{3}{2} \frac{\omega}{e^2} \varepsilon_0^2 y^2 g_2 (T_\omega - T_m)$, and by replacing T_m with \bar{T} and ε_0 with ε_a , $\overline{\Delta Q} = \frac{3}{2} \frac{\omega}{e^2} \varepsilon_a^2 y^2 g_2 (T_\omega - \bar{T})$. $\overline{\Delta Q} - \overline{\Delta Q}^{st}$ is calculated after substitution of ε_a by $\varepsilon_0 + \delta\hat{\varepsilon} \exp \nu t$ and \bar{T} by $T_m + \delta\hat{T} \exp \nu t$ and using of the definition (3.3) of a^2 :

$$\frac{\overline{\Delta Q} - \overline{\Delta Q}^{st}}{k} = a^2 y^2 \left[\left(1 + \frac{\delta\hat{\varepsilon}}{\varepsilon_0} \exp \nu t \right)^2 \left(T_\omega - (T_m + \delta\hat{T}(y) \exp \nu t) \right) - (T_\omega - T_m) \right].$$

This expression is approached at the first order by

$$\frac{\overline{\Delta Q} - \overline{\Delta Q}^{st}}{k} = a^2 y^2 \left[\left(1 + 2 \frac{\delta\hat{\varepsilon}}{\varepsilon_0} \exp \nu t \right) \left((T_\omega - T_m) - \delta\hat{T}(y) \exp \nu t \right) - (T_\omega - T_m) \right],$$

$$\frac{\overline{\Delta Q} - \overline{\Delta Q}^{st}}{k} = a^2 y^2 \left[2 \frac{\delta\hat{\varepsilon}}{\varepsilon_0} (T_\omega - T_m) - \delta\hat{T}(y) \right] \exp \nu t,$$

from which the result (5.9) follows.

Appendix B.

Using (3.11) and the fact that ε_0 and T_m have been replaced respectively by ε_a and \bar{T} , the bending moment is expressed as $M_a = \sqrt{M_1^2 + M_2^2} =$

$$12 \frac{l}{e} \varepsilon_a \left[\left(\int_0^e G'(\omega, \bar{T}) y^2 dy \right)^2 + \left(\int_0^e G''(\omega, \bar{T}) y^2 dy \right)^2 \right]^{1/2}.$$

After substitution of ε_a by $\varepsilon_0 + \delta\hat{\varepsilon} \exp \nu t$ and \bar{T} by $T_m + \delta\hat{T} \exp \nu t$ and development to the first order we have:

$$M_a = 12 \frac{l}{e} (\varepsilon_0 + \delta\hat{\varepsilon} \exp \nu t) \left[\left(\int_0^e G'(\omega, T_m) y^2 dy - \int_0^e h_2 \delta\hat{T} y^2 dy \exp \nu t \right)^2 + \left(\int_0^e G''(\omega, T_m) y^2 dy - \int_0^e g_2 \delta\hat{T} y^2 dy \exp \nu t \right)^2 \right]^{1/2}.$$

After factorisation by

$$M_0 = 12 \frac{l}{e} \varepsilon_0 \left[\left(\int_0^e G'(\omega, T_m) y^2 dy \right)^2 + \left(\int_0^e G''(\omega, T_m) y^2 dy \right)^2 \right]^{1/2},$$

we obtain:

$$M_a = M_0 \left(1 + \frac{\delta\hat{\varepsilon}}{\varepsilon_0} \exp \nu t \right) \times \left[1 - 2 \frac{\left[\int_0^e (h_2 G'(\omega, T_m) + g_2 G''(\omega, T_m)) y^2 dy \right] \left[\int_0^e \delta\hat{T} y^2 dy \right]}{\left[\left(\int_0^e G'(\omega, T_m) y^2 dy \right)^2 + \left(\int_0^e G''(\omega, T_m) y^2 dy \right)^2 \right]} \exp \nu t \right]^{1/2},$$

which is simplified as

$$M_a = M_0 \left(1 + \frac{\delta\hat{\varepsilon}}{\varepsilon_0} \exp \nu t \right) \times \left[1 - \frac{\left[\int_0^e (h_2 G'(\omega, T_m) + g_2 G''(\omega, T_m)) y^2 dy \right] \left[\int_0^e \delta\hat{T} y^2 dy \right]}{\left[\left(\int_0^e G'(\omega, T_m) y^2 dy \right)^2 + \left(\int_0^e G''(\omega, T_m) y^2 dy \right)^2 \right]} \exp \nu t \right].$$

This expression is developed at the first order as:

$$M_a = M_0 + M_0 \exp \nu t$$

$$\times \left[\frac{\delta \hat{\varepsilon}}{\varepsilon_0} - \frac{\left[\int_0^e (h_2 G'(\omega, T_m) + g_2 G''(\omega, T_m)) y^2 dy \right] \left[\int_0^e \delta \hat{T} y^2 dy \right]}{\left[\left(\int_0^e G'(\omega, T_m) y^2 dy \right)^2 + \left(\int_0^e G''(\omega, T_m) y^2 dy \right)^2 \right]} \right].$$

As a consequence,

$$\delta \hat{M} = M_0 \left[\frac{\delta \hat{\varepsilon}}{\varepsilon_0} - \frac{\left[\int_0^e (h_2 G'(\omega, T_m) + g_2 G''(\omega, T_m)) y^2 dy \right] \left[\int_0^e \delta \hat{T} y^2 dy \right]}{\left[\left(\int_0^e G'(\omega, T_m) y^2 dy \right)^2 + \left(\int_0^e G''(\omega, T_m) y^2 dy \right)^2 \right]} \right].$$

For a prescribed moment $\delta \hat{M} = 0$, we have

$$\frac{\delta \hat{\varepsilon}}{\varepsilon_0} = \frac{\left[\int_0^e (h_2 G'(\omega, T_m) + g_2 G''(\omega, T_m)) y^2 dy \right] \left[\int_0^e \delta \hat{T} y^2 dy \right]}{\left[\left(\int_0^e G'(\omega, T_m) y^2 dy \right)^2 + \left(\int_0^e G''(\omega, T_m) y^2 dy \right)^2 \right]}.$$

Appendix C.

Using the expression (3.1) of the dissipated energy $\langle \overline{\Delta Q}^{st} \rangle$ per cycle for a stationary process, we obtain by spacial averaging through the cross-sectional area:

$$(C.1) \quad \langle \overline{\Delta Q}^{st} \rangle = \frac{ke^2 a^2}{3} (T_\omega - T_m).$$

For a non-stationary process, the averaged dissipated energy $\langle \overline{\Delta Q} \rangle$ is obtained from spatial averaging of $\overline{\Delta Q}$. This result is obtained from (C1) by replacing T_m with \bar{T} and ε_0 with ε_a

$$(C.2) \quad \langle \overline{\Delta Q} \rangle = \frac{ke^2 a^2}{3} \left(1 + \frac{\delta \bar{\varepsilon}}{\varepsilon_0} \right)^2 (T_\omega - (T_m + \delta \bar{T}(t))).$$

At the first order, the expression (5.22) follows.

References

1. I. CONSTABLE, J.G. WILLIAMS and D.J. BURNS, *Fatigue and cyclic thermal softening of thermoplastics*, J. Mech. Engng Sci, **12**, 20–29, 1970.
2. R.M. CHRISTENSEN, *Theory of viscoelasticity*, Academic Press, 208–209, 1971.
3. F. DINZART and A. MOLINARI, *Cyclic torsion of a polymeric tube: self-heating and thermal failure*, J. of Thermal Stresses, **21**, 851–879, 1998.
4. J.D. FERRY, *Viscoelastic properties of polymers*, John Wiley, 1980.
5. R.W. HERTZBERG, *Deformation and fracture mechanics of engineering materials*, John Wiley, 1976.
6. N.C. HUANG and E.H. LEE, *Thermomechanical coupling behavior of viscoelastic rods subjected to cyclic loading*, J. of Applied Mechanics, 127–132, 1967.
7. G. MENGES and E. ALF, *Creep, self-heating and failure of thermoplastics under pulsating tensile stress*, J. of Elastomers and Plastics, **7**, 47–64, 1975.
8. S.B. RATNER and V.I. KOBOROV, *Self heating of plastics during cyclic deformation*, Mekh. Polymerov, **1**, 63–67, 1965.
9. M.N. RIDELL, G.P. KOO, J.L. O'TOOLE, *Fatigue mechanisms of thermoplastics*, Polym. Engng. Sci., **6**, 363–370, 1966.
10. A. TAKAHARA, K. YAMADA, T. KAJIYAMA, and M. TAKAYANAGI, *Evaluation of fatigue lifetime and elucidation of fatigue in plasticized Polyvinyl chloride in terms of dynamic viscoelasticity*, J. Appl. Polym. Sci., **25**, 597–614, 1980.
11. A. TAKAHARA, K. YAMADA, T. KAJIYAMA, and M. TAKAYANAGI, *Analysis of fatigue behavior of high-density polyethylene based on dynamic viscoelastic measurements during the fatigue process*, J. Appl. Polym. Sci., **26**, 1085–1104, 1981.
12. A. MOLINARI and Y. GERMAIN, *Self-heating and thermal failure of polymers sustaining a compressive cyclic loading*, Int. J. Solids, Structures, **33**, 23, 3439–3462, 1996.
13. Y.M. LEROY and A. MOLINARI, *Stability of steady states in shear zones*, J. Mech. Phys. Solids, **40**, 659–670, 1992.
14. Y.M. LEROY and A. MOLINARI, *Spatial patterns and size effects in shear zone: a hyperbolic model with higher-order gradients*, J. Mech. Phys. Solids, **41**, 4, 631–663, 1993.
15. G.A. LESIEUTRE and K. GOVINDSWAMY, *Finite element modeling of frequency dependent and temperature dependent dynamic behavior of viscoelastic materials in simple shear*, Int. J. Solids, Structures, **33**, 3, 419–432, 1996.
16. R.A. SCHAPERY, *Effect of cyclic loading on the temperature in viscoelastic media with variable properties*, AIAA Journal, **2**, 827–835, 1964.
17. R.A. SCHAPERY and D.E. CANTEY, *Thermomechanical response studies of solid propellants subjected to cyclic loading and random loading*, AIAA Journal, **2**, 827–835, 1964.
18. T.R. TAUCHERT, *The temperature generated during torsional oscillations of polyethylene rods*, Int. J. of Eng. Sciences, **5**, 353–365, 1967.
19. E.C. TING, *Heat generated in a torsional spring subjected to sinusoidal oscillations*, J. of Sound and Vibration, **22**, 81–92, 1972.

20. E.C. TING and J.L. TUAN, *Effect of internal pressure on the temperature distribution in a viscoelastic cylinder*, Int. J. of Mech. Sciences, **15**, 861–871, 1973.
21. A. WINEMAN and R. KOLBERG, *Response of beams of non-linear viscoelastic materials exhibiting strain-dependent stress relaxation*, Int. J. Non-Linear Mechanics, **32**, 5, 863–883, 1997.
22. I.S. GRADSHTEYN and I.M. RYZHIK, *Table of integrals series and products*, Academic Press, 1965.
23. G.N. WATSON, *A treatise on the theory of Bessel functions*, Cambridge University Press, 1966.

Received May 7, 2007; revised version January 17, 2008.
